Temperature- and Pressure-Dependent Phase Behavior of Monoacylglycerides Monoolein and Monoelaidin

C. Czeslik,* R. Winter,* G. Rapp,[‡] and K. Bartels[§]

*University of Dortmund, Institute of Physical Chemistry I, D-44221 Dortmund; [‡]European Molecular Biology Laboratory, Hamburg Outstation at DESY, D-22603 Hamburg; and [§]Berlin Neutron Scattering Center, Hahn-Meitner-Institut, D-14109 Berlin, Germany

ABSTRACT   We used x-ray and neutron diffraction to study the temperature- and pressure-dependent structure and phase behavior of the monoacylglycerides 1-monoelaidin (ME) and 1-monoolein (MO) in excess water. The monoacylglycerides were chosen for investigation of their phase behavior because they exhibit mesomorphic phases with one-, two-, and three-dimensional periodicity, such as lamellar, an inverted hexagonal and bicontinuous cubic phases, in a rather easily accessible temperature and pressure range. We studied the structure, stability, and transformations of the different phases over a wide temperature *and* pressure range, explored the epitaxial relations that exist between different phases, and established a relationship between the chemical structure of the lipid molecules and their phase behavior. For both systems, a temperature-pressure phase diagram has been determined in the temperature range from 0 to 100°C at pressures from ambient up to 1400 bar, and drastic differences in phase behavior are found for the two systems. In MO-water dispersions, the cubic phase Pn3m extends over a large phase field in the T,p-plane. At temperatures above 95°C, the inverted hexagonal phase is found. In the lower temperature region, a crystalline lamellar phase is induced at higher pressures. The phases found in ME-water include the lamellar crystalline L_c phase, the L_β gel phase, the L_α liquid-crystalline phase, and two cubic phases belonging to the crystallographic space groups Im3m and Pn3m. In addition, the existence of metastable phases has been exploited. Between coexisting metastable cubic structures, a metric relationship has been found that is predicted theoretically on the basis of the curvature elastic energy approximation only.

INTRODUCTION

Although most lipids in excess water exist in lamellar bilayer phases, certain lipids, including monoacylglycerides, can form nonbilayer hexagonal (H_{II}) or cubic liquid-crystalline phases as well (Cevc and Marsh, 1987; Andersson et al., 1988; Lindblom and Rilfors, 1989; Hyde, 1989; Seddon et al., 1990; Seddon, 1990; Tate et al., 1991; Cevc, 1993; Seddon and Templer, 1993; Briggs and Caffrey, 1994). Most of the cubic liquid-crystalline phases are now known to consist of bicontinuous regions of water and hydrocarbon, which can be described by infinite periodic minimal surfaces (IPMSs). An IPMS is an intersection-free surface periodic in three dimensions with a mean curvature that is everywhere zero. The surface, which sits at the lipid bilayer midplane, separates two interpenetrating but not connected water networks.

Nonlamellar phases, which occur for a number of membrane lipids, probably play an important functional role in some cell processes as local and transient intermediates (Mariani et al., 1988; Seddon, 1990; Boulignand, 1990; Tate et al., 1991). For example, cubic structures seem to be involved in membrane fusion, fat digestion, and might occur in intracellular organelles. Evidence also seems to consolidate that microorganisms control the lipid composition of their membranes to maintain them close to a composition

where nonlamellar structures would begin to appear (Lindblom et al., 1986).

Although some knowledge about the temperature- and water concentration-dependent phase behavior of lipid systems also exhibiting nonlamellar phases is available, almost nothing is known about the pressure-dependent phase behavior of these systems (Chang and Yager, 1983; So et al., 1993; Winter et al., 1994). Besides the general physicochemical interest in high pressure phase behavior and structure of amphiphilic molecules, high pressure is also of considerable physiological interest (Rostain et al., 1989; Balny et al., 1992). Furthermore, studies of pressure effects on lipid systems often led to the discovery of new phases and helped to understand the mechanisms underlying lipid phase transformations.

The monoacylglycerides 1-monoolein (C18:1c9) and 1-monoelaidin (C18:1t9) were chosen for investigation of their high pressure phase behavior because they exhibit mesomorphic phases with different lattice dimensionality at rather moderate conditions of temperature and pressure. Furthermore, their physico-chemical properties have received considerable interest because of their importance as intermediates in fat digestion and metabolism and because of their applications in food industry. The chemical structure and configuration of the two molecules are displayed in Fig. 1. These are neutral lipids, and the *cis* double-bond of MO and the *trans* double-bond of ME are located at the 9,10-position of their acyl chain. The temperature-water concentration phase diagrams of MO and ME have been established (Lutton, 1965; Hyde and Andersson, 1984; Caffrey, 1987).

In this study, mesomorphic phase identification of these systems is obtained from small-angle neutron diffraction and
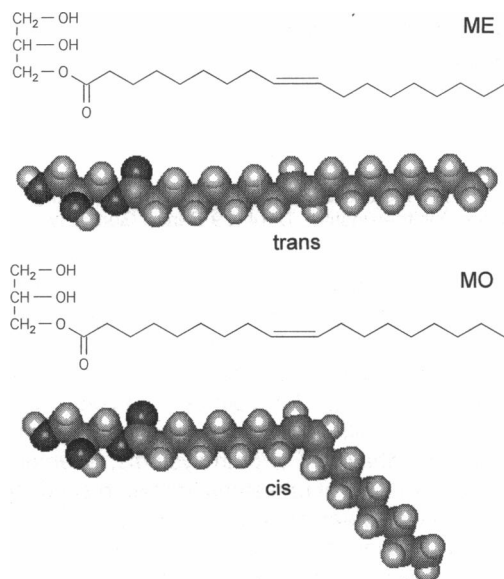
FIGURE 1 Chemical structure and conformation of ME and MO.

by both small- and wide-angle x-ray diffraction using synchrotron radiation, and changes in the diffraction patterns indicate lipid phase transformations. From these studies, temperature-pressure phase diagrams have been established for MO and ME in excess water in the temperature range from 0 to 100°C at pressures from ambient up to 1400 bar. Such studies are very useful in analyzing the underlying mechanisms of lipid phase transitions, and in proving theoretical models for the energetics of lipid structures and the mesophase behavior of lipid systems. Additionally, the existence of metastable and undercooled phases has been exploited.

MATERIALS AND METHODS

The monoacylglycerides 1-monoelaidin and 1-monoolein were obtained from Sigma Chemical Co. (Deisenhofen, Germany). They had a purity of >99% and were used without further purification. Aqueous dispersions of 10–30 wt% lipid were prepared by weighing the appropriate amounts of lipid and bidistilled H_2O (or D_2O for the neutron diffraction experiments), and the samples were subjected to three freeze-thaw vortex cycles.

The calorimetric measurements were performed on a Perkin-Elmer DSC7 differential scanning calorimeter (DSC). The lipid mixtures (in H_2O or D_2O) were filled into stainless steal pans. The samples were heated at a programmed heating rate of 1°C/min. To evaluate the phase transition temperatures, a straight line was fitted to the upward deflection of the DSC transition curve. The transition enthalpies, ΔH_{tr}, were evaluated from the areas under the calorimetric curves.

The small- and wide-angle x-ray diffraction experiments were performed at the beam line X13 of the EMBL outstation at DESY. With the germanium monochromator used, the wavelength was fixed to 1.5 Å. Sets of tungsten slits were used to adjust the beam size at the sample (~0.5 mm in height and 4 mm in width) and to reduce parasitic scattering. One-dimensional diffraction patterns were recorded using a sealed linear detector with delay line readout. The diffraction patterns in the small- and wide-angle regime were recorded simultaneously using two detectors connected in series (Rapp et al., 1995). The distance between the sample and the small-angle detector was 230 cm, and the sample to wide-angle detector distance was 50 cm. The samples were held in a thermostatically controlled sample holder

between two 25-μm-thick mica windows. The temperature was controlled to within 0.2°C. The reciprocal spacings $s = 1/d = (2/\lambda)\sin\theta$ (d = lattice spacing, 2θ = scattering angle, λ = wavelength of radiation) were calibrated in the small-angle region by the diffraction pattern of rat-tail collagen, whereas for the wide-angle region glycerol tripalmitate was used. The x-ray exposure time was 2–5 s/frame. To avoid radiation damage, a small selenoid-driven lead shutter protected the samples from excess radiation within the periods where no data were recorded. The high pressure x-ray cell for performing the pressure-dependent studies is described elsewhere (J. Erbes and R. Winter, unpublished data).

The small-angle neutron scattering experiments were performed at the BERII research reactor at the Hahn-Meitner-Institut using the V1 membrane diffractometer. A neutron wavelength of 5.8 Å was used, and a Be filter suppressed higher order wavelengths. The sample to ${}^3He$ detector distance was 100 cm. It took about 15 min to record one diffractogram with good statistics for the integrated intensities. The high pressure cell used for the pressure-dependent studies has been described in detail elsewhere (Winter et al., 1991).

RESULTS

MO-water

DSC measurements of MO-H_2O dispersions in excess water exhibit a phase transition at $T = 95°C$. According to the literature, the transition is due to the conversion of a cubic primitive (with crystallographic space group Pn3m) to an inverted hexagonal (H_{II}) phase (Hyde and Andersson, 1984; Caffrey, 1987). The enthalpy change ΔH_{tr} calculated from the DSC trace for the cubic to the H_{II} phase transition is very small, about 0.3 kJ/mol, which is a typical value for phase transition enthalpies between phases with fluid-like hydrocarbon chains. The transition temperature of a MO-D_2O dispersion is shifted 9°C toward lower temperatures. ΔH_{tr} of this system is about 0.2 kJ/mol. The differences in the phase transition temperature and the enthalpy change observed for the two lipid dispersions might be due to the different strengths of hydrogen bonding in H_2O and D_2O at the lipid headgroup.

The x-ray diffraction measurements of MO-H_2O dispersions were performed in the temperature range from 5 to 100°C. Selected diffraction patterns in the small- and wide-angle diffraction region are given in Fig. 2. Below 95°C, the
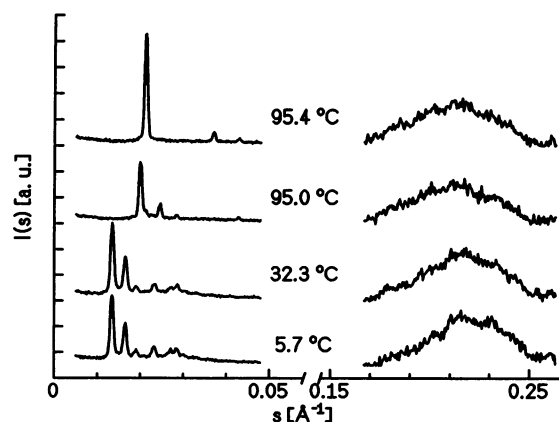

FIGURE 2 X-ray small- and wide-angle scattering intensity $I(s)$ of a 20 wt% MO-H_2O dispersion at selected temperatures.

Bragg reflections of a cubic structure are seen in the small-angle region, which can be indexed as (110), (111), (200), (211), (220), and (221) reflections on a cubic lattice of space group Pn3m. The lattice spacing is 105 Å at 5.7°C and 71 Å at 92°C. At about 95°C, the cubic phase transforms into a H_{II} phase. Recently, it has been shown by time-resolved x-ray diffraction that this transition appears to be a two-state transition (Caffrey, 1987). The three Bragg peaks observed above 95°C (see Fig. 2), which are spaced in the ratio 1: $\sqrt{3}$:2, correspond to the (10), (11), and (20) reflections of the H_{II} structure. The lattice constant a of the hexagonal phase (center-to-center distance of adjacent cylinders), which has been calculated from $s = (2/a \sqrt{3}) (h^2 + k^2 + hk)^{1/2}$ (h and k are Miller indices), is 54.6 Å at 95.4°C, which is similar to the value found by Caffrey (1987), and decreases at a rate of about −0.17 Å/°C with increasing temperature. This negative sign of the temperature lattice coefficient da/dT is essentially a consequence of the growing disorder within the chains, resulting in a larger splay of the chains and, thus, a smaller radius of the water core of the H_{II} structure. The broad wide-angle scattering peak reflects a disordered packing of the hydrocarbon chains, which is typical for fluid-like chains, in both lipid phases. The lattice constant increases linearly from about 4.5 Å at 5.7°C up to 4.7 Å at 95°C, because of a slight and monotonical reduction in lateral lipid packing. As can be seen from Fig. 3, the lattice constant of the cubic phase Pn3m stays about constant from 5 to 30°C, and then decreases with increasing temperature, $(da/dT)_{1bar} = -0.89$ Å/°C at 40°C, and $(da/dT)_{1bar} = -0.24$ Å/°C at 80°C. Interestingly, a similar form of the temperature dependence of the lattice parameter $a(T)$ of the cubic phase Pn3m has been found in DOPE-water dispersions recently (Erbes et al., 1994b). Within a cubic phase region of the phase diagram, increasing temperature generally leads to a decrease in unit cell size because of an increased curvature of the lipid bilayer. With increasing temperature, the bilayer gets thinner and the ratio between the minimal surface and

the parallel surface of the polar/nonpolar interface corresponds to an increased molecular wedge shape.

From high pressure small-angle neutron scattering experiments, the lattice parameter, and therefore the volume per unit cell, of the cubic phase is found to be strongly pressure-dependent. In Fig. 4, the pressure dependence of the (110) and (111) reflection of the cubic phase is seen at, e.g., $T = 50°C$. A value of $(da/dp)_{50°C} = 7.9$ Å/kbar has been found for $a(p)$. At $T = 20°C$, $(da/dp)_{20°C} = 7.3$ Å/kbar. Increasing pressure has the reverse effect on the lipid molecular shape as increasing temperature. Molecular wedge shape decreases, resulting in a decreased curvature of the bilayer and an enlargement of the unit cell size.

Assuming the lattice constant along the cubic to H_{II} phase boundary to be the same, a transition slope $(dT/dp)_{coex}$ of about 33°C/kbar is obtained for the cubic to H_{II} transition line. For comparison, the lamellar liquid-crystalline to H_{II} transition is more pressure-sensitive: $(dT/dp)_{coex} = 40°C/$kbar has been found in dioleoylphosphatidylethanolamine-water and egg-phosphatidylethanolamine-water dispersions (Chang and Yager, 1983; So et al., 1993; Landwehr and Winter, 1994).

From additional high pressure x-ray diffraction experiments at lower temperatures, a transition to a crystalline lamellar phase L_c has been observed. For example, at $T = 7.5°C$ and $p = 1400$ bar, a Bragg peak emerges at $s = 0.0212$ Å^{-1}, which corresponds to a lamellar lattice spacing of 47 Å. Multiple Bragg reflections occur in the wide-angle region. In passing from the Pn3m to the L_c phase, an intermediate lamellar phase with d-spacing of 43 Å is observed, which transforms into the crystalline lamellar phase within about 30 min. The temperature-pressure phase-diagram of MO in excess water in the temperature range from 0 to 100°C at pressures from ambient up to 1400 bar is depicted in Fig. 5. It can be seen clearly that the cubic primitive phase Pn3m extends over a remarkable large phase field in the T,p-plane.
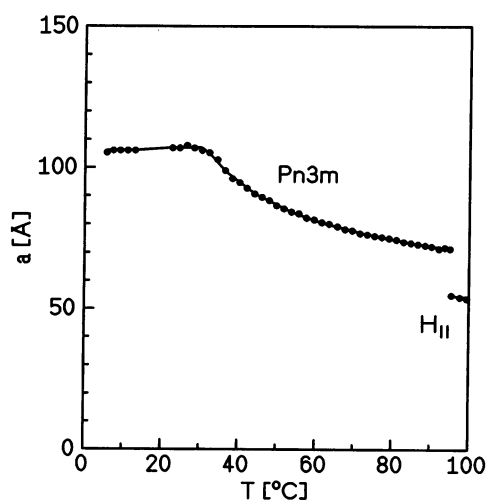

FIGURE 3   Lattice constant a of the cubic, and inverted hexagonal phase of MO in excess water as a function of temperature.
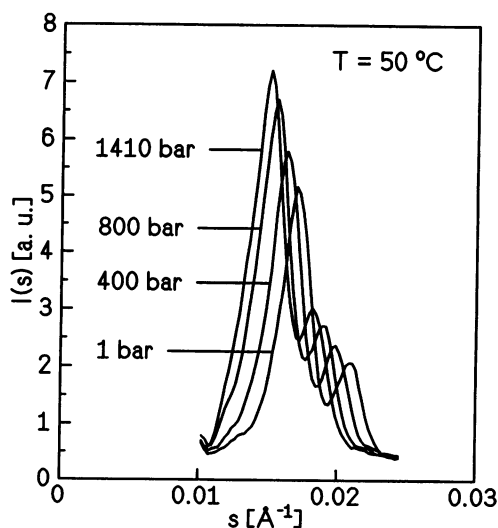

FIGURE 4   Small-angle neutron diffraction patterns of MO in excess water at $T = 50°C$ as a function of pressure.
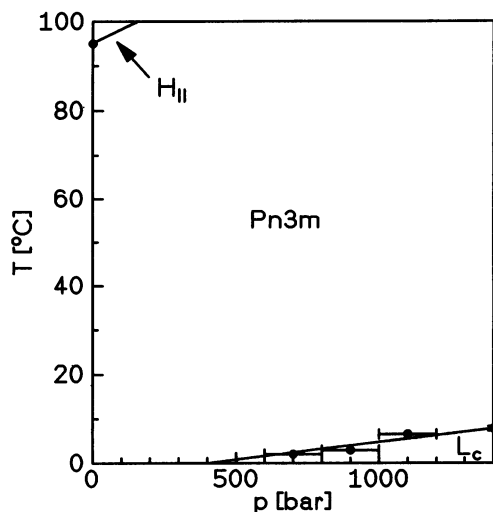
FIGURE 5   Temperature-pressure phase diagram of MO in excess water. Error bars for the transition pressures are indicated.

ME-water

The DSC scan for ME in excess water exhibits a phase transition at 21°C that is accompanied by an enthalpy change of 21 kJ/mol. The transition can be ascribed to a conversion from a lamellar gel (L_β) to a lamellar liquid-crystalline (L_α) structure (Caffrey, 1987). The L_β-L_α transition is entropy-driven, i.e., the introduction of *gauche* conformers into the lipid chains increases the amount of rotational isomerism and, hence, the configurational entropy of the chains. The corresponding transition in D_2O as solvent occurs at a temperature higher by 1.5°C with $\Delta H_{tr} = 18$ kJ/mol. In the temperature range from 40 to 60°C, additional very small and broad DSC peaks with enthalpy changes of roughly 0.1 kJ/mol have been observed. Their positions change according to the sample history, however. These transitions are due to the slow formation of different cubic phases, as will be shown below.

Fig. 6 displays selected small- and wide-angle x-ray diffraction patterns of a ME-H_2O dispersion in the temperature range from 10.8 to 73.7°C. In the low temperature phase at 10.8°C, the lamellar L_β gel phase exists with the lamellar repeat unit of 62.6 Å. The corresponding wide-angle region exhibits a single peak according to a hexagonal lipid packing with the lattice constant of 4.2 Å. Above 21°C, the lamellar liquid-crystalline L_α phase is formed, with the lattice constant of 52.3 Å at 29.8°C. The wide-angle region of the diffraction pattern reveals a diffuse scattering peak centered at ~4.5 Å^{-1}, indicating that the lipid acyl chains have undergone a melting transition and are now far more mobile.

Fig. 7 shows the SAXS pattern during a heating experiment when temperature was increased at a rate of 0.2°C/min from 35 to 49°C. At 39.4°C, a new phase is formed out of the L_α structure, as can be inferred from the occurrence of further reflections at small s values. They can be interpreted to arise from a mixture of the body-centered cubic phase Im3m with lattice parameter $a = 222$ Å and the cubic primi-
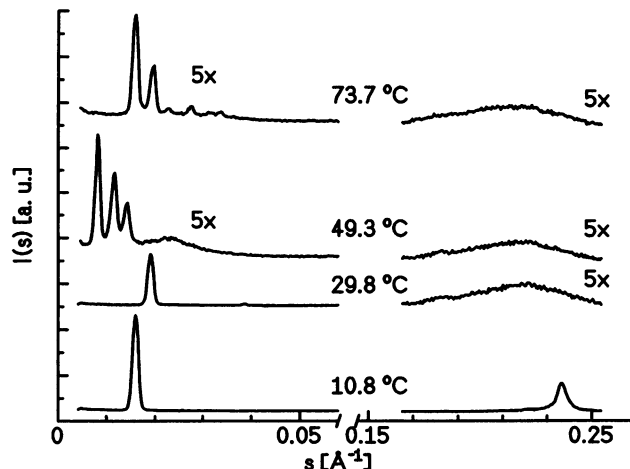

FIGURE 6   X-ray small- and wide-angle scattering intensity $I(s)$ of a 30 wt% ME-H_2O dispersion at selected temperatures.
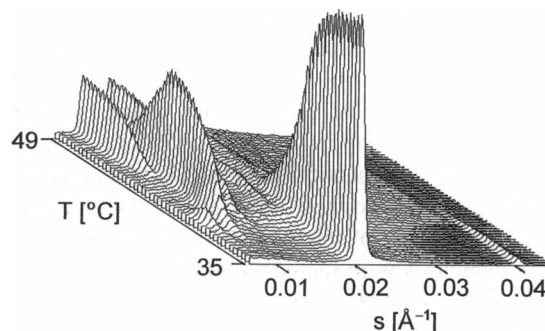

FIGURE 7   X-ray small-angle diffraction patterns of a 30 wt% ME-H_2O dispersion during a heating experiment from 35 to 49°C at a rate of 0.2°C/min.

tive phase Pn3m with a = 171 Å. A definite lattice assignment on so few orders of reflection is difficult, however. The fluidity and large size of the cubic lattice results in only a few orders of diffraction being detected. After an initial rise, the intensities of the Pn3m reflections drastically decrease with increasing temperature, leaving three reflections spaced in the ratio $\sqrt{2}:\sqrt{4}:\sqrt{6}$, which can be assigned to the body-centered lattice Im3m space group with a unit cell length of 171 Å at 49.3°C. One might speculate that the intermediate Pn3m cubic structure formed at 39.4°C is metastable, because its reflections fade with increasing temperature. Furthermore, after several weeks the Im3m phase only was observed in this intermediate temperature range. Indeed, it is a well known phenomenon that cubic phases exhibit metastable phase behavior, often complicating the identification of equilibrium states in hydrated lipid systems. A metric relation of about 1.28 between the repeat units of the two cubic lattices Im3m and Pn3m has been found. This metric relationship of the two cubic lattices has been found in other lipid systems as well (Hyde and Andersson, 1984; Erbes et al., 1994b), and has also been predicted theoretically. This prediction is based on the fact that the two cubic structures Im3m

and Pn3m with periodic minimal surfaces P (Schwarz' surface) and D (diamond type surface) (Andersson et al., 1988; Hyde and Andersson, 1984; Hyde, 1990) can be transformed into one another with no cost of curvature free energy by a surface transformation of the Bonnet type. At a temperature of 63.9°C, a different cubic phase emerges, with six orders of diffraction spaced in the ratio $\sqrt{2}:\sqrt{3}:\sqrt{4}:\sqrt{6}:\sqrt{8}:\sqrt{9}$. A space group consistent with orders spaced in these ratios is Pn3m with a 97.8 Å unit cell. Its lattice constant also decreases with increasing temperature and reaches 88.5 Å at $T = 73.7$°C. The broad wide-angle reflection has increased to about 4.6 Å^{-1} at this temperature. Thus, the following tentative phase sequence is obtained for ME in excess water as a function of temperature up to 93°C: L_β, L_α, Im3m, Pn3m. A similar temperature-dependent phase sequence has been found by Caffrey (1987), except for the intermediate phase, which has not been addressed in the literature so far. This phase sequence in ME-water is thus much more complex than that of the corresponding lipid with an oleoyl chain, the difference being solely due to the difference in double-bond configuration of the two lipid molecules. With MO, the Pn3m phase extends over a wide temperature range and passes through the H_{II} phase upon heating.

Fig. 8 displays the lattice constants of the different structures of ME-H_2O at ambient pressure as a function of temperature. The lattice constant in the lamellar gel phase increases linearly with 0.24 Å/°C. The positive temperature coefficient might be due to an increase in water hydration of the lipid headgroup. The lattice constant in the wide-angle region increases at a rate of 0.003 Å/°C. The repeat unit of the lamellar liquid-crystalline phase decreases with -0.12 Å/°C, which is most likely due to increasing temperature-induced *gauche* conformers in the acyl chains. The Im3m- and also the "metastable" intermediate Pn3m-cubic structure exhibits a strong temperature-dependent lattice parameter in the temperature range from 40 to 63°C, e.g., $(\mathrm{d}a/\mathrm{d}T) = -3.1$

Å/°C at $T = 54$°C. Although the thermal lattice coefficient of the cubic phases in this temperature range is very large, $\mathrm{d}a/\mathrm{d}T$ of the Pn3m cubic structure above 63°C is considerably smaller: $(\mathrm{d}a/\mathrm{d}T) = -0.66$ Å/°C. The large temperature coefficient of the two coexisting cubic lattices, as compared with that of the pure cubic phase Pn3m at higher temperatures, might also partially reflect the relative changes in phase composition of the two competing cubic structures with increasing temperature.

All of the data shown above have been taken in the heating direction at a rate of 0.2°C/min. Upon reducing the temperature from 65°C at a rate of -0.5°C/min, undercooling phenomena occur and metastable cubic phases are found. The Pn3m phase is found to be metastable down to 27°C, and the Im3m structure is observed only between 29 and 21°C. Further lowering the temperature results in the L_β gel phase formation, leaving out the lamellar liquid-crystalline phase. Indeed, cubic phases are well known to be notorious for their tendency to undercool. Presumably, upon cooling the cubic phases cannot access easily the desired larger lattice parameters because of a kinetically limited uptake of water. As noted by Luzzati (Luzzati et al., 1986), cubic phase metastability might also be important in biological systems.

Pressure-dependent measurements on ME dispersions have been performed using x-ray and neutron diffraction. As an example, Fig. 9 displays selected SAXS patterns at $T = 65$°C as a function of pressure. At pressures above $\sim$300 bar, the cubic primitive phase Pn3m ($a = 97.8$ Å) has transformed into the cubic body-centered phase Im3m ($a = 145$ Å). At 1400 bar, the phase transition to the lamellar liquid-crystalline L_α phase with repeat unit of 50.6 Å has taken place. The pressure dependence of the lattice parameter, $a(p)$, of the cubic phase Pn3m has been determined for several temperatures. One finds a linear increase of $a(p)$, e.g., $(\mathrm{d}a/\mathrm{d}p)_{80°C} = 15$ Å/kbar for $T = 80$°C. High pressure SANS measurements at 13°C revealed that a phase transition occurs in the L_β gel phase (lattice spacing 61.4 Å) around 700 bar.
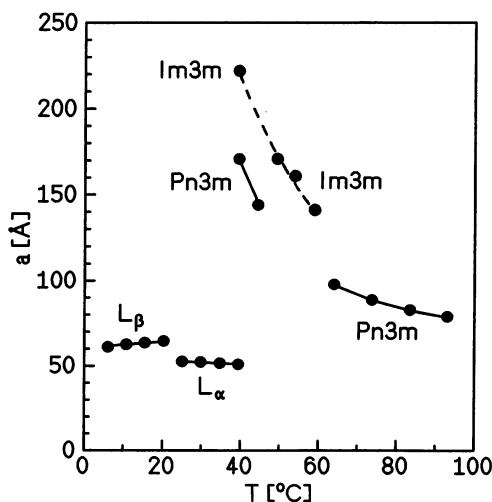

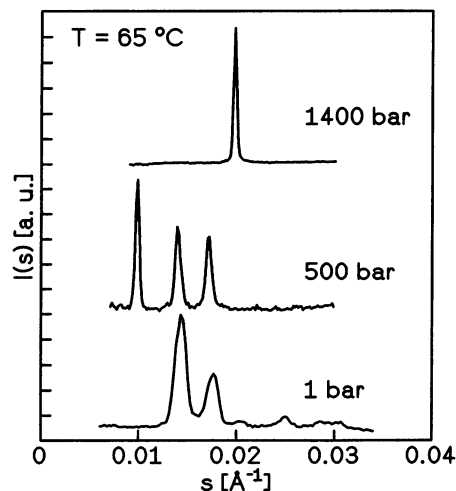FIGURE 8   Lattice constants of the lamellar and cubic phases of ME in excess water as a function of temperature.

FIGURE 9   Small-angle x-ray diffraction patterns of ME in excess water at $T = 65$°C as a function of pressure.

The newly discovered phase is probably a crystalline lamellar L_c phase with lattice constant of 51 Å. Recently, a crystalline lamellar structure with a small lamellar repeat period of 50 Å has also been found in ME samples dehydrated by high osmotic pressure (McIntosh et al., 1989). To establish the T,p-phase diagram of ME-H_2O, a series of x-ray diffraction experiments was carried out for pressures from 1 to 1000 bar at temperatures ranging from 0 to 85°C. The phases identified and their locations in the temperature-pressure space are shown in Fig. 10. Metastable phases are not shown in the diagram. The phases found in ME-water include the lamellar crystalline L_c phase, the L_β gel phase, the L_α liquid-crystalline phase, and two cubic phases belonging to the crystallographic space groups Im3m and Pn3m. The phase boundaries of the various transitions exhibit a similar slope, which seems to slightly decrease with increasing pressure. At lower temperatures and high pressures, the lamellar gel and crystalline structures are being formed, because of their smaller partial molar lipid volumes.

The data shown above were taken at constant pressure in the heating direction. Similar to the finding, that metastable cubic phases are formed upon cooling the sample at ambient pressure, metastable phases are also found in ME-H_2O by increasing the pressure at constant temperature. For example, at $T = 58°C$, the intercubic phase transformation from the Pn3m to the Im3m structure takes place at pressures above 1000 bar.

DISCUSSION

The stability of the lamellar phases of ME at lower temperatures over the cubic and inverted hexagonal phase, as compared with MO, might be explained by very simple molecular packing arguments, as introduced by Israelachvili (1992). He defined a so-called packing parameter $\eta = V/A_o l_c$, where V is the volume of the hydrocarbon chains, l_c is the maximum effective hydrocarbon chain length, and A_o is the optimal surface area per molecule defined at the polar/nonpolar interface. When lipids, for which $\eta \approx 1$, are dispersed in excess water, lamellar structures are generally found. As the value of η increases, the molecule becomes more wedge-shaped, and there is an increasing tendency of the molecules to aggregate into structures with negative curvatures, such as the inverted cubic and hexagonal phases. The monoacylglycerides possess small polar head groups. The cross sectional area occupied by the lipid headgroup is probably smaller compared with that of the partially bent chain of MO (see Fig. 1), thus giving the molecule an overall conical shape. By exchanging the cis double-bond of MO with the trans double-bond of ME, the length of the chains becomes larger, so that the average molecular shape is more cylindrical. Thus, the observed increased stability of the planar lamellar phases in ME as compared with MO can be understood in this qualitative way.

The change in molecular wedge shape by temperature and pressure might also qualitatively explain part of the observed temperature-pressure phase diagrams of the lipid systems. An increased wedge shape from the polar head toward the methyl end of the lipid molecules is a result of heating, and pressure has the opposite effect, because increase of pressure increases the lipid chain order parameter (Winter and Pilgrim, 1989; Jonas, 1993). Andersson et al. (1988) showed that the topology of bicontinuous cubic phases can in certain cases result in a lower free energy than that of either the lamellar or H_{II} phase, and cubic phases do not suffer this extreme chain packing stress of the H_{II} phase. When the wedge shape increases with temperature in MO, strain is built up in the cubic structure, which ultimately results in a phase transition to the H_{II} structure, as the gain in curvature free energy in the H_{II} state overcompensates its higher chain packing energy. Applying pressure thus has the opposite effect and leads to the transformation of the H_{II} to the cubic phase. Upon further increasing the pressure, a more cylindrical lipid molecular shape is obtained that finally leads to the formation of a lamellar phase at lower temperatures with its higher lipid packing density.

In the lower temperature region of the T,p-phase diagram of ME-H_2O, the phase sequence as a function of pressure is, as expected, L_α-L_β-L_c, due to the decreasing partial molar lipid volumes in this series (Wiener et al., 1988; Böttner et al., 1994). The L_β-L_c- transition curve has a slope of about 20°C/kbar. For the L_α-L_β transition line, a slope of 20°C/kbar is also found, which is similar to that of the corresponding phospholipid system dielaidoylphosphatidylcholine (Winter and Pilgrim, 1989), thus demonstrating that the lamellar liquid-crystalline to gel main transition is governed by the "melting" of the acyl chains, with the headgroup interactions being of less importance. Interestingly, the other transitions between lipid structures with fluid-like chains also exhibit a similar slope. Assuming also a first-order transition for the cubic-L_α and the intercubic Pn3m-Im3m phase transformation, and noting that ΔH_{tr} is smaller than 0.1 kJ/mol in these cases, this might be explained by a rather small volume change in the course of these phase transformations. Dilatometric measurements are underway to settle this question.
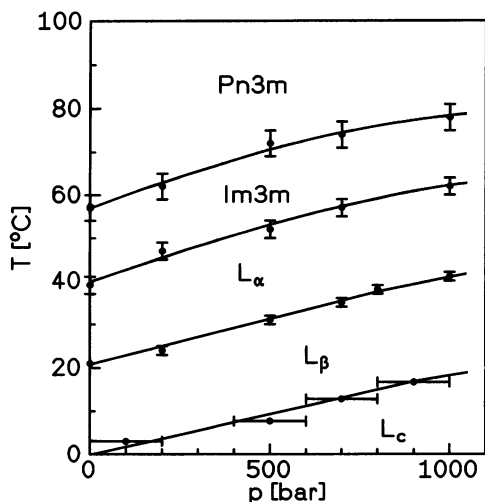

FIGURE 10 Temperature-pressure phase diagram of ME in excess water.

Although the local geometry and topology of the P and D periodic minimal surfaces are similar, which means that the energetic minima for their curvature free energies are the same, the experimental data show that the symmetry of the cubic structure observed depends on temperature and pressure. It is clear that an understanding of the form of the phase diagram would require a detailed consideration of all of the complex interactions involved, such as interfacial, hydration and Van der Waals forces, steric repulsion, hydrogen bonding etc., as well as the structure of the lipid molecule as a function of the thermodynamic parameters temperature and pressure. At present, there is still much debate concerning the modeling of some of these contributions, however (Seddon and Templer, 1993; Chung and Caffrey, 1994; Templer et al., 1994) and, thus, one is not yet able to predict the cubic phase stability and intercubic phase sequence as a function of temperature and pressure. The experimental data presented might help, however, to disentangle different free energy contributions in further theoretical approaches.

REFERENCES

Andersson, S., S. T. Hyde, K. Larsson, and S. Lidin. 1988. Minimal surfaces and structures: from inorganic and metal crystals to cell membranes and biopolymers. *Chem. Rev.* 88:221–242.

Balny, C., R. Hayashi, K. Heremans, and P. Masson, editors. 1992. High Pressure and Biotechnology, Vol. 224. Colloque Inserm. John Libbey Eurotext, Montrouge, France.

Böttner, M., D. Ceh, U. Jacobs, and R. Winter. 1994. High pressure volumetric measurements on phospholipid bilayers. *Z. Phys. Chem.* 184:205–218.

Boulignand, Y. 1990. Comparative geometry of cytomembranes and water-lipid systems. *J. Physiol. (Paris).* 51:35–52.

Briggs, J., and M. Caffrey. 1994. The temperature-composition phase diagram of monomyristolein in water: equilibrium and metastabililty aspects. *Biophys. J.* 66:573–587.

Caffrey, M. 1987. Kinetics and mechanism of transitions involving the lamellar, cubic, inverted hexagonal, and fluid isotropic phases of hydrated monoacylglycerides monitored by time-resolved x-ray diffraction. *Biochemistry.* 26:6349–6363.

Cevc, G. 1993. Phospholipids Handbook. Marcel Dekker, New York.

Cevc, G., and D. Marsh. 1987. Phospholipid Bilayers. John Wiley & Sons, New York.

Chang, E. L., and P. Yager. 1983. Effect of high pressure on a lipid non-bilayer phase. *Mol. Cryst. Liq. Cryst.* 98:125–129.

Chung, H., and M. Caffrey. 1994. The curvature elastic-energy function of the lipid-water cubic mesophase. *Nature.* 368:224–226.

Erbes, J., C. Czeslik, W. Hahn, M. Rappolt, G. Rapp, and R. Winter. 1994b. On the existence of bicontinuous cubic phases in dioleoylphosphatidylethanolamine. *Ber. Bunsen-Ges. Phys. Chem.* 98:1287–1293.

Hyde, S. T. 1989. Microstructure of bicontinuous surfactant aggregates. *J. Phys. Chem.* 93:1458–1464.

Hyde, S. T. 1990. Curvature and the global structure of interfaces in surfactant-water systems. *J. Physique Colloque C7.* 51:209–228.

Hyde, S. T., and S. Andersson. 1984. A cubic structure consisting of a lipid bilayer forming an infinite periodic minimum surface of the gyroid type in the glycerolmonooleat-water system. *Z. Kristallogr.* 168:213–219.

Israelachvili, J. N. 1992. Intermolecular and Surface Forces. Academic Press, New York.

Jonas, J. 1993. High pressure NMR studies of chemical and biochemical systems. *In* High Pressure Chemistry, Biochemistry, and Material Science. R. Winter and J. Jonas, editors. Kluwer Academic Publishers, Dordrecht. 393–442.

Landwehr, A., and R. Winter. 1994. High-pressure differential thermal analysis of lamellar to lamellar and lamellar to non-lamellar lipid phase transitions. *Ber. Bunsen-Ges. Phys. Chem.* 98:214–218.

Lindblom, G., and L. Rilfors. 1989. Cubic phases and isotropic structures formed by membrane lipids: possible biological relevance. *Biochim. Biophys. Acta.* 988:221–256.

Lindblom, G., I. Brentel, M. Sjölund, G. Wikander, and A. Wieslander. 1986. Phase equilibria of membrane lipids from Acholeplasma laidlawii. The importance of a single lipid forming non-lamellar phases. *Biochemistry.* 25:7502–7510.

Lutton, E. S. 1965. Phase behavior of aqueous systems of monoglycerides. *J. Am. Oil Chem. Soc.* 42:1068–1070.

Luzzati, V., A. Gulik, T. Gulik-Krzywicki, and A. Tardieu. 1986. *In* Lipids and Membranes: Past, Present and Future. J. A. F. Op den Kamp, B. Roelofsen, and K. W. A. Wirtz, editors. Elsevier, Amsterdam. 137–151.

Mariani, P., V. Luzzati, and H. Delacroix. 1988. Cubic phases of lipid-containing systems: structure analysis, and biological implications. *J. Mol. Biol.* 204:165–189.

McIntosh, T. J., A. D. Magid, and S. A. Simon. 1989. Repulsive interactions between uncharged bilayers: hydration and fluctuation pressures for monoglycerides. *Biophys. J.* 55:897–904.

Rapp, G., A. Gabriel, M. Dosière, and H. J. Koch. 1995. A dual detector single readout system for simultaneous small- (SAXS) and wide-angle X-ray (WAXS) scattering. *Nucl. Instrum. Methods.* In press.

Rostain, J. C., E. Martinez, and C. Lemaire, editors. 1989. High Pressure Nervous Syndrome: 20 Years Later. ARAS-SNHP Publications, Marseille, France.

Seddon, J. M. 1990. Structure of the inverted hexagonal (H$_{II}$) phase, and non-lamellar phase transitions of lipids. *Biochim. Biophys. Acta.* 1031:1–69.

Seddon, J. M., and R. H. Templer. 1993. Cubic phases of self-assembled amphiphilic aggregates. *Phil. Trans. R. Soc. Lond. A Math. Phys. Sci.* 344:377–401.

Seddon, J. M., J. L. Hogan, N. A. Warrender, and E. Pebay-Peyroula. 1990. Structural studies of phospholipid cubic phases. *Progr. Colloid Polymer Sci.* 81:189–197.

So, P. T. C., S. M. Gruner, and E. S. Shyamsunder. 1993. Pressure-induced topological phase transitions in membranes. *Phys. Rev. Lett.* 70:3455–3458.

Tate, M. W., E. F. Eikenberry, D. C. Turner, E. Shyamsunder, and S. M. Gruner. 1991. Nonbilayer phases of membrane lipids. *Chem. Phys. Lipids.* 57:147–164.

Templer, R. H., J. M. Seddon, and N. A. Warrender. 1994. Measuring the elastic parameters for inverse bicontinuous cubic phases. *Biophys. Chem.* 49:1–12.

Wiener, M. C., S. Tristram-Nagle, D. A. Wilkinson, L. E. Campbell, and J. F. Nagle. 1988. Specific volumes of lipids in fully hydrated bilayer dispersions. *Biochim. Biophys. Acta.* 938:135–142.

Winter, R., and W.-C. Pilgrim. 1989. A SANS study of high pressure phase transitions in model biomembranes. *Ber. Bunsen-Ges. Phys. Chem.* 93:708–717.

Winter, R., M.-H. Christmann, M. Böttner, P. Thiyagarajan, and R. Heenan. 1991. The influence of the local anaesthetic tetracaine on the temperature and pressure dependent phase behaviour of model biomembranes. *Ber. Bunsen-Ges. Phys. Chem.* 95:811–820.

Winter, R., A. Landwehr, T. Brauns, J. Erbes, C. Czeslik, and O. Reis. 1994. High pressure effects on the structure, and phase behavior of model membrane systems. *In* Proceedings of the 23rd Steenbock Symposium on "High Pressure Effects in Molecular Biophysics and Enzymology." Madison, WI.